Investigation of spray-coated silver-microparticle electrodes for ionic electroactive polymer actuators

Catherine Meis, Nastaran Hashemi, and Reza Montazami

Articles you may be interested in

Multiphysics of ionic polymer–metal composite actuator
J. Appl. Phys. **114**, 084902 (2013); 10.1063/1.4818412

Mechanical characterization of an electrostrictive polymer for actuation and energy harvesting
J. Appl. Phys. **111**, 124115 (2012); 10.1063/1.4729532

Thickness dependence of curvature, strain, and response time in ionic electroactive polymer actuators fabricated via layer-by-layer assembly
J. Appl. Phys. **109**, 104301 (2011); 10.1063/1.3590166

Magnetically actuated microrotors with individual pumping speed and direction control
Appl. Phys. Lett. **95**, 023504 (2009); 10.1063/1.3176969

Micromechanics of actuation of ionic polymer-metal composites
J. Appl. Phys. **92**, 2899 (2002); 10.1063/1.1495888

Investigation of spray-coated silver-microparticle electrodes for ionic electroactive polymer actuators

Catherine Meis,[1] Nastaran Hashemi,[2] and Reza Montazami[2,a)]

[1]Department of Materials Science and Engineering, Iowa State University, Ames, Iowa 50011, USA
[2]Department of Mechanical Engineering, Iowa State University, Ames, Iowa 50011, USA

We have employed the easy-to-scale-up method of spray-coating in combination with layer-by-layer self-assembly technique to fabricate ionic electroactive polymer actuators (IEAPAs). IEAPAs with spray-coated silver microparticle electrodes demonstrate enhanced strain and response time when compared to nearly identical, optimized conventional IEAPA with gold leaf electrodes. The results demonstrate that strain of these IEAPAs increases with the decrease of thickness of the outer silver microparticle electrodes. In addition, the response time of the actuators at frequencies of 1 and 10 Hz improves compared to optimized conventionally fabricated IEAPA. It was found that samples consisting of spray-coated silver electrodes can charge up to $\sim$3 times faster than conventional actuators at 1 Hz frequency. Faster charging/discharging results in higher mobility of ions within the actuator and thus, faster actuation. Given the relatively large thickness of the silver microparticle electrodes ($\sim$50$\times$ gold leaf), similar strain was observed due to the lower Young's modulus of spray-coated layers compared to that of bulk material. © 2014 AIP Publishing LLC. [http://dx.doi.org/10.1063/1.4870181]

I. INTRODUCTION

Stimuli responsive materials have attracted considerable interest from the materials research community. Unique properties of stimuli responsive materials have made this class of materials the backbone of many fascinating ideas such as drug delivery vehicles, artificial skin, artificial muscles, smart windows, etc.[1–8] Electroactive polymers (EAPs) are soft, flexible and low-density functional materials that exhibit response to electrical stimulant. Electromechanical EAPs are a class of EAPs that exhibit mechanical response to external electrical stimulus. Electromechanical response of EAPs can be explained by either electrostatic force (dielectric EAPs) or displacement of ions inside the polymer matrix (ionic EAPs (IEAPs)).[9,10] In recent years, IEAPs have increasingly been researched and developed for a wide variety of applications, such as microrobotics, artificial muscles, on-chip fluid mixing, smart skins, sensors, and actuators, to name a few.[11–17] Also of increasing importance today is the ability of fabrication techniques to be translated into manufacturing to allow these new materials, structures and devices to be commercially produced.[18,19]

Generally, IEAP actuators (IEAPAs) are constructed of an ion-doped ionic polymer-metal composite (IPMC) sandwiched between two conductive electrodes. The IPMC itself consists of an ionomeric membrane, typically nafion, with thin layers of conductive network composite (CNC) deposited on both sides.[20,21] IPMCs have been manufactured from a variety of methods, but more common methods include electroless plating and impregnation-reduction.[22,23] Recently, Akle *et al.* developed the direct assembly process or DAP for the complete fabrication of ionic polymer transducers; the process

is unique for allowing considerable flexibility in materials and design.[24] In our previous studies, we, for the first time, employed the layer-by-layer or LbL fabrication technique to deposit thin films of gold nanoparticles (AuNPs) as CNC layers onto the ionomeric membrane to form the IPMC. We demonstrated that high performance actuators can be fabricated with this technique.[25] Therefore, LbL is the method we have chosen to fabricate the CNC layers for the actuators investigated in this report, while spray coating is employed to fabricate the outer electrodes.

Previous studies have demonstrated the great influence of CNC layers on the electromechanical behavior of IEAP actuators; moreover, it is well known that the dynamics of mobility and diffusion of ions in IPMC and their interaction with CNC layers have a vital rule in defining the electromechanical properties of ionic devices.[26–28]

We have previously shown that higher strain and bending curvature can be achieved by employing the LbL technique with AuNPs to form porous CNC layers of desired physical properties.[25,29] One of the main advantages of using the LbL technique is the ability to construct electrically conductive, porous CNCs while keeping the thickness in the nanometer range.[5,30,31] Such ultra-thin composites do not interfere with the desired mechanical properties of the nafion membrane. That is, the modulus is not changed by a significant amount, while the CNC–ion interface is dramatically increased, and mobility of ions through the CNC is facilitated. Moreover, IPMCs with porous CNC layers have larger electrolyte uptake capacity due to their high porosity. Previously, we have shown that the thickness of the CNC is highly influential on the performance of IEAP actuators.[9] In that prior work, we demonstrated that increasing the thickness of the CNC results in larger strain and bending curvature, which are the results of the increased electrolyte uptake, without significantly increasing the overall thickness or modulus of the IPMC.

a)Author to whom correspondence should be addressed. Electronic mail: reza@iastate.edu

Much research has been done regarding different materials and methods for the portion of the electrode that is adhered directly onto the ionomeric membrane itself, but not regarding the outer electrode. Contact electrodes are typically applied as the outermost layer of IEAP actuators to increase performance.[32] It has been shown that adding a thin metal electrode, typically gold, enhances performance because the metal lowers the surface resistance.[24] Akle *et al.* have developed a few different application methods for outer electrodes as part of their DAP process.[24] For water hydrated IPMCs, one method was to add a platinum layer by impregnation-reduction and then electroplate a thin gold layer on top; the second method was to apply gold in self-assembled monolayer through light etching lithography. Another method is to hot-press gold leaf onto the surface of the IPMC; several other researchers have also used this method with a variety of EAP devices.[9,20,24,33]

The main purpose of the outer electrodes for IPMCs is to increase performance by efficiently distributing electrical stimulus across the entire surface area of material. Factors to consider regarding outer electrode materials and application method include the material thickness necessary to produce an adequately conductive surface and the interaction of the electrode material with the CNC layer and ionomeric membrane. Additionally, the outer electrode material must be light-weight so the actuator can support and move its own mass, adhere to the membrane to provide sufficient electrical connection, and be flexible to withstand repeated back-and-forth bending motion. Material structures with lower Young's modulus are desired to minimize internal mechanical resistance to bending. Generally, due to their microstructure, spray-coated layers have lower Young's modulus compared to the bulk material.[34,35] As presented in Figure 1(a), the IEAPAs utilized for this study consist of five layers, two of which are the outer electrodes responsible for providing uniform electric field across the actuator when

stimulated; the two CNC layers and the internal ionomeric membrane comprise the remaining three layers. High conductivity of the outer electrodes is essential in defining the response time and actuation speed of the IEAPA, while their thickness is a limiting factor as it adds to the rigidity of the device. Optimized electromechanical response can be achieved by increasing the conductivity of the electrodes, while maintaining relatively small thicknesses. This leads to light and flexible IEAPAs with short charge/discharge times.

In this work, we investigate the performance of IEAPAs with outer silver electrodes that have been applied via spray deposition in comparison with the same IEAPAs with hot-pressed gold leaf electrodes. Spray application method for the silver electrodes provides good adhesion to the nafion membrane and CNC layers, resulting in more stable IEAPAs, and is also a relatively fast and easy process with high manufacturing potentials. We have quantified the frequency dependence of the strain of the resultant actuators with different outer electrode thicknesses.

II. EXPERIMENTAL

Commercially available 25 μm thick nafion (NR-211, Ion Power, Inc.) was utilized as the ionomeric membrane in all IEAPAs fabricated for this study. The CNCs consisted of alternating layers of the polycation poly(allylamine hydrochloride) (PAH, Sigma Aldrich) and gold nanoparticles dispersed in aqueous solution (AuNPs, ~3 nm diameter, 20 ppm, Purest Colloids, Inc.). The CNC layers were deposited as an ionically self-assembled thin-film onto the nafion through the LbL process, using a StrataSequence 6 robotic multilayering device (NanoStrata, Inc). The specifics of the LbL process for this particular application have been described in our previous works;[9,20] briefly, the nafion film was cut and secured on glass frames using double-sided tape, substrates were alternately immersed for 5 min each in aqueous solutions of PAH at a
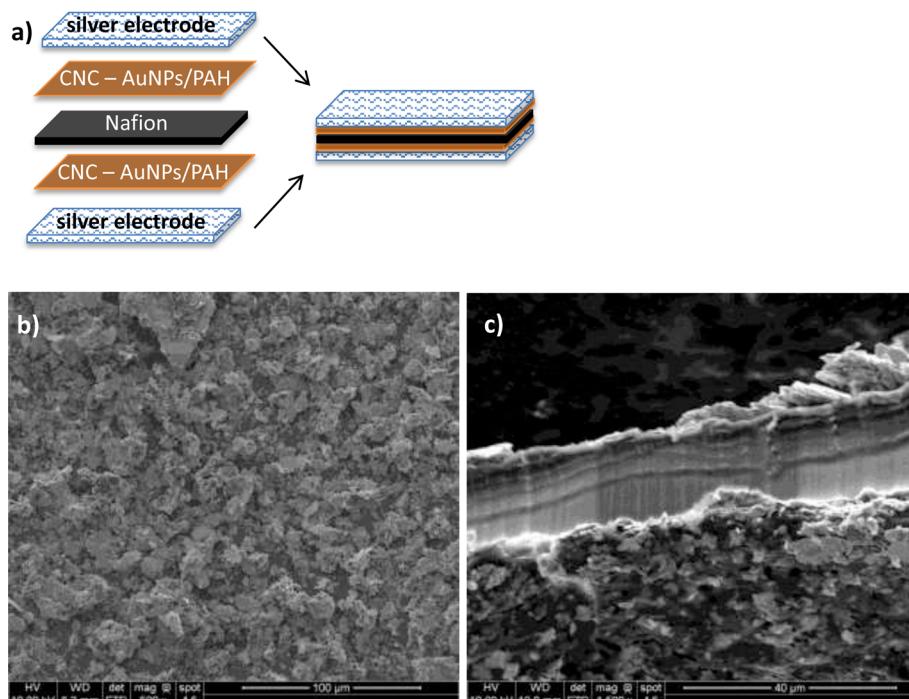
FIG. 1. (a) Schematic of components and completely assembled actuator (not to scale). (b) SEM image of the silver electrode surface verifying uniform deposition. (c) SEM image of the cross-section of a completely assembled actuator, each of the different component layers are clearly visible: Silver electrodes, CNC layer, and nafion.

concentration of 10 mM at pH 4.0 and AuNPs at 20 ppm concentration at pH 9.0 with three rinsing steps for 1 min each in deionized water after each deposition step to form one bilayer. All samples studied in this work consisted of 20 bilayers of AuNPs/PAH. Following deposition of the CNC layers, the membranes were soaked in 1-ethyl-3-methylimidazolium trifluoromethanesulfonate (EMI-Tf) (Sigma Aldrich) ionic liquid at 80 °C to approximately 40 wt. %; excess EMI-Tf was carefully removed by pressing the membrane with a piece of soft filter paper. Outer electrodes were fabricated on IPMCs via either spray-coated silver or hot pressed gold leaf (50 nm thick). For silver electrodes, conductive silver paste (PELCO) in form of finely dispersed silver microparticles in an acrylic resin was diluted in acetone to 25% of its original concentration and was applied for electrodes. The silver paste was diluted to minimize excess weight to allow the IEAPAs to function with characteristic high strain and fast response while still providing a uniform conductive surface. After the excess ionic liquid was removed, a small air compressor in combination with gravity feed airbrush with a 0.2 mm nozzle, set at 20 psi operating pressure, was used to spray the diluted silver paste onto the membranes. In order to vary electrode thickness, samples were fabricated with both single and double layers of silver paste deposited for the electrodes; different thicknesses of single layer electrodes were also fabricated by varying the deposition speed. For gold electrodes, gold leaf was hot-pressed at 90 °C under 220 psi for 20 s. The thicknesses of different samples are presented in Table I.

The actuators were cut into approximately 1×10 mm^2 strips for testing purposes. The 4-point-probe method with collinear probe arrangement was used to measure and calculate sheet resistance. Sheet resistance calculations were performed using the following equation:

$$R_s = 4.53 \times \frac{V}{I}, \tag{1}$$

where R_s is sheet resistance ($\Omega/\square$), V is the voltage (mV), I is current (mA), and 4.53 is the correction factor due to small sample size and consequent edge effects.

The thickness of the silver electrode layers was measured from scanning electron microscopy (SEM) images of the cross section of the films. Standard electrochemistry experiments were conducted on both the gold leaf and spray-coated silver microparticle electrodes to test for surface reactions. According to the results of cyclic voltammetry measurements, there do not appear to be significant chemical reactions occurring on either of the electrode surfaces, within the operation range (± 4 V) of the actuators. Electrical stimulus (4 V square waveform) was provided by a function generator and monitored using a digital

phosphor oscilloscope. A charge-coupled device (CCD) camera, mounted to an in-house made micro-probe station, recorded actuation at a rate of 30 fps. Subsequent video analysis yielded radius of curvature r or tip displacement δ of the free end of the actuator, depending on if the material flexed to a large extent or produced a more vibration-like motion, respectively. Net strain percentage $\varepsilon(\%)$ was calculated using two different methods, again depending on the extent of flexing. For significant flexing, the following equation was used:

$$\varepsilon(\%) = \frac{h}{2r} \times 100, \tag{2}$$

where r is the radius of curvature and h the thickness of the actuator.[20] For very minimal (vibration-like) flexing, the following equation was used:

$$\varepsilon(\%) = \frac{\delta h}{L^2} \times 100, \tag{3}$$

where δ is the tip displacement and L is the free length of the actuator.[20,24]

III. RESULTS AND DISCUSSION

A. IEAPA characteristics

The spray-coating method we utilized allowed us to produce thin, light, and uniform silver electrodes on the surface of the IPMC, which is critical to the functionality of the actuators. Actuation depends largely on the uniform distribution of electrical charge across the surface area of the entire actuator; thus, imperfections in the outer conductive surface have significant impact on the overall function of the actuator. Since actuation occurs due to the motion of ions through the CNC layers and the nafion, it follows that uniform electric charge will result in uniform and simultaneous motion of ions and causes the entire actuator to bend evenly along its length. The complete structure of the ionic electroactive polymer actuators, with silver electrodes, is shown in detail in Fig. 1.

The IEAPAs fabricated via LbL fabrication process have been shown to produce higher strains and bending curvatures than similar IEAPAs fabricated using alternative methods.[25] Based on our previous studies, thicker[9] and more closely-packed[20] CNC layers exhibit higher strains and bending curvatures. In addition, we have shown previously that denser CNCs charge and discharge at a faster rate, which translates to faster actuation speed and smaller time constants. In this work we examined samples with CNC layers consisting of 20 closely-packed bilayers of AuNP/PAH; this configuration was chosen based on previous studies.[9,20,25] The CNC layer, while also highly conductive, functions as a reservoir for the ionic liquid and as a porous material through which ions can migrate. It follows that a thick, dense active CNC layer with pores large enough to allow the passage of ions, in combination with thinner external outer electrodes, will result in optimum efficiency. Taking into account the approximate two-dimensional geometry of the IPMCs, with thickness significantly smaller than width and length, the

TABLE I. Thickness of different components of variety of actuators.

Sample	CNC (μm)	IPMC (μm)	Outer electrode (μm)	Actuator (μm)
Au	0.040	25.08	0.050	25.18
Ag1	0.040	25.08	2.75	30.58
Ag2	0.040	25.08	3.80	32.68
Ag3	0.040	25.08	6.67	38.42

sheet resistance of IPMC consisting of 20 bilayers of AuNP/PAH was measured using the four-point-probe method (Eq. (1)). The measurements were carried out under 20–120 mV, using very low current flow (10–100 nA) to compensate for the relatively high resistance of the thin films. The sheet resistance of the IPMC was measured to be 1.31 MΩ/□, which is significantly smaller than that of uncoated nafion (50.48 MΩ/□).

We also experimented with dip-coating the IPMCs into diluted conductive silver to fabricate the outer electrodes, but the nafion absorbed the solvent and then crinkled. This resulted in pooling of the silver particles in the remaining solvent, causing significant variations in the thickness of the silver electrode so that portions of the surface were not conductive. Crinkling of the nafion due to absorption of solvents has also been mentioned by Akle et al.[24] However, when the conductive silver was sprayed onto the IPMC, the solvent dried quickly enough that it was not absorbed by the nafion, and the samples remained flat and uniform. SEM images were taken from the cross-section of actuators consisting of different thickness outer electrodes. The thicknesses of the outer electrodes were then deduced from the cross-section images. Data regarding the thickness of components of each IEAPA are presented in Table I. We expect that there is some limit where the outer electrode thickness is small enough that the sheet resistance becomes quite significant, causing actuator performance to decrease.

B. Mechanical response

The sheet resistance of the silver electrode material is reported to be 0.015 Ω/□/25 μm (∼0.0006 Ω/□/μm). Considering the application method, the actual sheet resistance value for the spray-coated electrode layers may be slightly higher than the given value; the spray coating produced a uniform layer of silver flakes (Fig. 1), so any discrepancy is simply due to the morphology and structure of the silver microparticle layer. However, the potential higher resistance inherent to using silver microparticles as the outer electrode does not seem to significantly impede the bending curvature or tip displacement.

Electromechanical response of the actuators was measured and recorded under application of a 4 V square wave at various frequencies. Strain values were calculated using measured radius of curvature (Eq. (2)) for frequency of 0.1 Hz, and tip displacement (Eq. (3)) for frequencies of 1 and 10 Hz.

As presented in Figure 2, at low frequency of 0.1 Hz, samples consisting of thinner silver electrodes (i.e., Ag1 and Ag2) exhibited strains comparable to that of Au sample. Both Ag1 and Ag2 samples exhibited 0.47% strain, which is barely more than 0.46% strain of the Au sample. It is expected that greater strains occur at low frequencies because the electrodes have enough time to fully charge; thus, ions have more time to migrate through the internal structure of the nafion and CNC layers to accumulate at the oppositely charged electrodes, causing larger bending curvature. It is anticipated that the ions in sample Ag3 have also
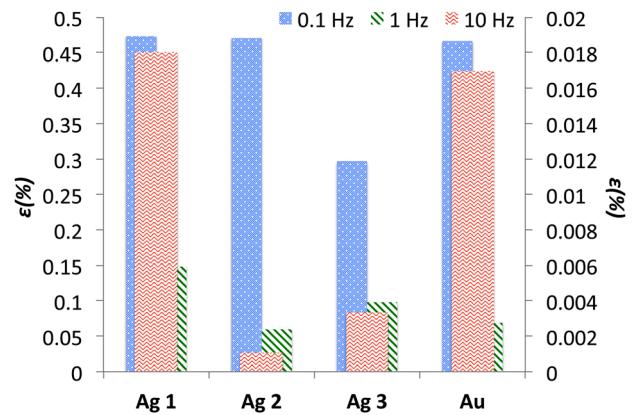
FIG. 2. Net strain percentage ε(%) as a function of frequency using a 4 V square wave function. Data presented for gold and varying silver electrode thicknesses. 10 Hz data are presented vs. the secondary y-axis.

accumulated at the oppositely charged electrodes; however, the generated strain was not enough to fully compensate the increased stiffness due to the added thickness. Given that the Au sample is an optimized sample, it is particularly interesting that the thin Ag samples, at low frequency, functioned comparably to their gold electrode counterpart. We believe that the performance of Ag samples could be increased by fabrication of even thinner electrodes, if the conductivity can be maintained. Utilizing thinner electrodes reduces both stiffness and mass of the actuators; thus, reduces the force wasted within the actuator.

At an order of magnitude higher frequency (1 Hz), the strain values dropped by several folds; however, overall, the Ag1 sample exhibited superior performance compared to Au and other Ag samples. While the strain of the Au sample dropped by 6.5 folds (0.46% to 0.07%), that of Ag1 sample dropped by only 3.3 folds (0.47% to 0.14%). The evidence suggests that the Ag1 outer electrodes can reach approximately 33% of full charge capacity in approximately 10% of time required for fully charging the electrodes, when the Au sample can only reach about 15% of the full charge capacity in the same duration of time. Presented in Figure 3 is
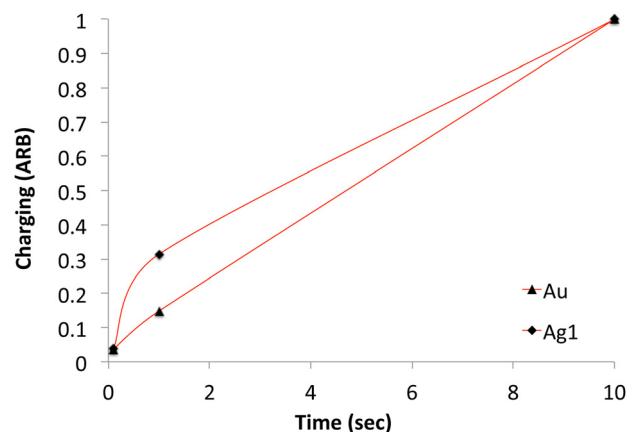
FIG. 3. Normalized charging of the Au and Ag1 IEAPA as a function of time. The lines are to guide the eye and were extrapolated between the three marked data points, which correlate to the charging in arbitrary units (ARB) at three distinct frequencies: 10 Hz, 1 Hz, and 0.1 Hz. These are the three distinct frequencies shown in Fig. 2, encompassing the range of frequencies tested in this study.

normalized charging of the two thinnest samples (Au and Ag1) as a function of time.

Samples Ag2 and Ag3 did not exhibit a substantial strain at significantly faster frequency of 10 Hz. Since both samples are relatively thick and thus stiff, the stress generated by the very limited number of ions that have reached the oppositely charged electrodes at the short period of 100 ms is not enough to significantly bend the structure. The thinner Ag1 and Au samples showed a strain drop of approximately 27 folds (compare to 0.1 Hz); yet, the vibration-like bending was still noticeable in both cases. Ag1 and Au samples showed strains of 0.018% and 0.017%, respectively. This suggests that both samples charge to about the same level of 3.7% in the first 1% of time required to fully charge (10 s).

IV. CONCLUSION

We have successfully fabricated IEAPA with spray-coated silver outer electrodes, with minimum influence on the electromechanical performance of the devices; and, have demonstrated that the IEAPA fabricated with this easy-to-scale-up method can exhibit comparable performance to IEAPA fabricated with ultra-thin gold-leaf electrodes. It was observed that IEAPA consisting of a relatively thin spray-coated electrode is capable of generating higher strain at a faster rate. The maximum strain generated by this actuator (Ag1) was barely more than that of an optimized conventional actuator (Au); when the time constant of the Ag1 is shorter than that of Au sample. The improved response time and strain achieved in this work are results of successful fabrication of thin, yet highly conductive outer electrodes with low Young's modulus due to the use of spray-coating.

[1]S. Giri, B. G. Trewyn, M. P. Stellmaker, and V. S. Y. Lin, "Stimuli-responsive controlled-release delivery system based on mesoporous silica nanorods capped with magnetic nanoparticles," Angew. Chem. Int. Ed. **44**(32), 5038–5044 (2005).

[2]Y. Zhu, J. Shi, W. Shen, X. Dong, J. Feng, M. Ruan et al., "Stimuli-responsive controlled drug release from a hollow mesoporous silica sphere/-polyelectrolyte multilayer core–shell structure," Angew. Chem. **117**(32), 5213–5217 (2005).

[3]Y. Qiu and K. Park, "Environment-sensitive hydrogels for drug delivery," Adv. Drug Delivery Rev. **53**, 321–339 (2012).

[4]J. Kost and R. Langer, "Responsive polymeric delivery systems," Adv. Drug Delivery Rev. **64**, 327–341 (2012).

[5]R. Montazami, V. Jain, and J. R. Heflin, "High contrast asymmetric solid state electrochromic devices based on layer-by-layer deposition of polyaniline and poly(aniline sulfonic acid)," Electrochim. Acta **56**(2), 990–994 (2010).

[6]V. Jain, H. M. Yochum, R. Montazami, and J. R. Heflin, "Millisecond switching in solid state electrochromic polymer devices fabricated from

[7]ionic self-assembled multilayers," Appl. Phys. Lett. **92**(3), 033304 (2008).

[7]V. Jain, H. Yochum, H. Wang, R. Montazami, M. Hurtado, A. Mendoza-Galvan et al., "Solid-state electrochromic devices via ionic self-assembled multilayers (ISAM) of a polyviologen," Macromol. Chem. Phys. **209**(2), 150–157 (2008).

[8]V. Jain, M. Khiterer, R. Montazami, H. Yochum, K. Shea, and J. Heflin, "High-contrast solid-state electrochromic devices of viologen-bridged polysilsesquioxane nanoparticles fabricated by layer-by-layer assembly," ACS Appl. Mater. Interfaces **1**(1), 83–89 (2009).

[9]R. Montazami, S. Liu, Y. Liu, D. Wang, Q. Zhang, and J. R. Heflin, "Thickness dependence of curvature, strain, and response time in ionic electroactive polymer actuators fabricated via layer-by-layer assembly," J. Appl. Phys. **109**(10), 104301 (2011).

[10]M. Shahinpoor and K. J. Kim, "Ionic polymer-metal composites: I. Fundamentals," Smart Mater. Struct. **10**(4), 819 (2001).

[11]M. Shahinpoor and K. J. Kim, "Ionic polymer–metal composites: III. Modeling and simulation as biomimetic sensors, actuators, transducers, and artificial muscles," Smart Mater. Struct. **13**(6), 1362 (2004).

[12]M. Shahinpoor and K. J. Kim, "Ionic polymer–metal composites: IV. Industrial and medical applications," Smart Mater. Struct. **14**(1), 197 (2005).

[13]Yoseph Bar-Cohen, Electroactive Polymer (EAP) Actuators as Artificial Muscles: Reality, Potential, and Challenges (SPIE press Bellingham, WA, 2004), Vol. 5.

[14]L. Ceseracciu, M. Biso, A. Ansaldo, D. N. Futaba, K. Hata, A. C. Barone et al., "Mechanics and actuation properties of bucky gel-based electroactive polymers," Sens. Actuators B **156**(2), 949–953 (2011).

[15]C. Murray, D. McCoul, E. Sollier, T. Ruggiero, X. Niu, Q. Pei et al., "Electro-adaptive microfluidics for active tuning of channel geometry using polymer actuators," Microfluid. Nanofluid. **14**(1–2), 345–358 (2013).

[16]Utilization of Electroactive Polymer Actuators in Micromixing and in Extended-life Biosensor Applications, SPIE Smart Structures and Materials + Nondestructive Evaluation and Health Monitoring, edited by V. Ho, M. Shimada, D. Szeto, X. C. i Solvas, D. Scott, L. S. Dolci et al., (International Society for Optics and Photonics, 2010).

[17]A. K. Price, K. M. Anderson, and C. T. Culbertson, "Demonstration of an integrated electroactive polymer actuator on a microfluidic electrophoresis device," Lab Chip **9**(14), 2076–2084 (2009).

[18]Z. Chen, T. I. Um, and H. Bart-Smith, "A novel fabrication of ionic polymer–metal composite membrane actuator capable of 3-dimensional kinematic motions," Sens. Actuators A **168**(1), 131–139 (2011).

[19]R. Tiwari and E. Garcia, "The state of understanding of ionic polymer metal composite architecture: A review," Smart Mater. Struct. **20**(8), 083001 (2011).

[20]R. Montazami, D. Wang, and J. R. Heflin, "Influence of conductive network composite structure on the electromechanical performance of ionic electroactive polymer actuators," Int. J. Smart Nano Mater. **3**(3), 204–213 (2012).

[21]M. D. Bennett and D. Leo, "Manufacture and characterization of ionic polymer transducers employing non-precious metal electrodes," Smart Mater. Struct. **12**(3), 424 (2003).

[22]K. J. Kim and M. Shahinpoor, "Ionic polymer–metal composites: II. Manufacturing techniques," Smart Mater. Struct. **12**(1), 65 (2003).

[23]M. Yu, H. Shen, and Z.-D. Dai, "Manufacture and performance of ionic polymer-metal composites," J. Bionic Eng. **4**(3), 143–149 (2007).

[24]B. J. Akle, M. D. Bennett, D. J. Leo, K. B. Wiles, and J. E. McGrath, "Direct assembly process: A novel fabrication technique for large strain ionic polymer transducers," J. Mater. Sci. **42**(16), 7031–7041 (2007).

[25]S. Liu, R. Montazami, Y. Liu, V. Jain, M. Lin, J. R. Heflin et al., "Layer-by-layer self-assembled conductor network composites in ionic polymer metal composite actuators with high strain response," Appl. Phys. Lett. **95**(2), 023505 (2009).

[26]B. J. Akle, M. D. Bennett, and D. J. Leo, "High-strain ionomeric-ionic liquid electroactive actuators," Sens. Actuators A **126**(1), 173–181 (2006).

[27]B. Akle, D. Leo, M. Hickner, and J. McGrath, "Correlation of capacitance and actuation in ionomeric polymer transducers," J. Mater. Sci. **40**(14), 3715–3724 (2005).

[28]M. Shahinpoor and K. Kim, "Novel ionic polymer-metal composites equipped with physically loaded particulate electrodes as biomimetic sensors, actuators and artificial muscles," Sens. Actuators A **96**(2–3), 125–132 (2002).

[29]S. Liu, R. Montazami, Y. Liu, V. Jain, M. Lin, X. Zhou et al., "Influence of the conductor network composites on the electromechanical

performance of ionic polymer conductor network composite actuators," Sens. Actuators A **157**(2), 267–275 (2010).

[30]G. Decher, "Fuzzy nanoassemblies: Toward layered polymeric multi-composites," Science **277**(5330), 1232–1237 (1997).

[31]P. Hammond, "Form and function in multilayer assembly: New applications at the nanoscale," Adv. Mater. **16**(15), 1271–1293 (2004).

[32]M. Shahinpoor and K. J. Kim, "The effect of surface-electrode resistance on the performance of ionic polymer-metal composite (IPMC) artificial muscles," Smart Mater. Struct. **9**(4), 543 (2000).

[33]V. Palmre, E. Lust, A. Jänes, M. Koel, A.-L. Peikolainen, J. Torop *et al.*, "Electroactive polymer actuators with carbon aerogel electrodes," J. Mater. Chem. **21**(8), 2577–2583 (2011).

[34]C. Li, A. Ohmori, and R. McPherson, "The relationship between microstructure and Young's modulus of thermally sprayed ceramic coatings," J. Mater. Sci. **32**(4), 997–1004 (1997).

[35]Y. Tsui, C. Doyle, and T. Clyne, "Plasma sprayed hydroxyapatite coatings on titanium substrates Part 1: Mechanical properties and residual stress levels," Biomaterials **19**(22), 2015–2029 (1998).